ChemComm

COMMUNICATION

View Article Online
View Journal | View Issue

Cite this: *Chem. Commun.*, 2022, **58**, 6498

Received 3rd April 2022,
Accepted 3rd May 2022

DOI: 10.1039/d2cc01908f

rsc.li/chemcomm

Stereoelectronically-induced allosteric binding: shape complementarity promotes positive cooperativity in fullerene/buckybowl complexes†

Eric S. Larsen, [ab] Guillermo Ahumada, [a] Prakash R. Sultane [a] and Christopher W. Bielawski *[ab]

A novel 2 : 1 host–guest complex forms between 8-*tert*-butyl-6*b*^{2}-azapenta-benzo[*bc*,*ef*,*hi*,*kl*,*no*]corannulene (1) and C_{60} with positive cooperativity (α = 2.56) and high affinity ($K_1 \times K_2 = 2.8 \times 10^6$ M^{-2}) at 25 °C. The C_{60} undergoes increasing shape complementarity toward 1 throughout the binding process.

The discovery of the fullerenes[1] prompted efforts toward finding applications for the novel carbon allotrope, ranging from photovoltaics,[2,3] and organic electronics[4] to medicine[5,6] and self-assembly.[7] A landmark demonstration[8] of the latter was reported by Wennerström who showed that a host–guest complex forms between C_{60} and γ-cyclodextrin. Since then, the field[9–11] has progressed toward achieving selective fullerene complexation to not only expedite isolation and purification[12–15] but to also facilitate the construction of organized nanostructures.[16–20] The formation of stable assemblies is apropos to achieving these aims and a broad variety of molecular components have been explored for their abilities to form complexes with fullerenes, including calixarenes,[21] tetrathiafulvalenes,[22,23] subphthalocyanines,[24] and porphyrins.[25,26]

Due to the complementarity of their respective concave and convex surfaces, bowl-shaped polycyclic aromatic hydrocarbons (PAHs) – often colloquially referred to as "buckybowls" – are prime candidates for forming assemblies with C_{60}.[25,27–29] For example, corannulene,[30] a prototypical buckybowl, has been shown to form a 1 : 1 complex with C_{60} that resembles a ball-and-socket joint (Fig. 1), albeit only in the solid state.[31,32] To enhance buckybowl-fullerene interactions, PAHs have been enlarged to increase surface area and/or modified with electron-rich components.[27] For example, association constant (K_a) values of up to 1400 M^{-1} were measured in solution (toluene-d_8) when corannulene was decorated with pendant arylthiol groups and then treated with C_{60}.[33,34] An even larger association constant was measured (6.2×10^4 M^{-1}, toluene) when corannulene was integrated with an electron-rich heteroatom (*i.e.*, azacorannulene) and then introduced to electron-deficient C_{60}.[35–38]

Binding enhancement has also been demonstrated by tethering multiple buckybowls in such a way that they become preorganized to chelate C_{60}.[27] For example, the "buckycatcher" consists of two corannulene units spanned across a tetrabenzocyclooctatetraene linker and acts as a type of molecular tweezer for C_{60} ($K_a = 2.7 \times 10^3$ M^{-1}, toluene-d_8).[39,40] Azacorannulene-based tweezers have also been synthesized and shown to display large association constants with C_{60} (up to 3.0×10^8 M^{-1} in toluene), depending on the linker used.[38] Despite the growing diversity, the majority of buckybowl-fullerene complexes can be classified as 1 : 1 host–guest systems. Multi-component assemblies comprised of multiple fullerene hosts and/or multiple buckybowls are relatively rare in solid[21,41–46] or solution states,[28,47,48] and typically utilize modified buckybowls or porphyrins. "Super-stoichiometric" complexes are attractive because they can be expected to exhibit relatively high stabilities and thus form with greater selectivity when compared to their stoichiometric analogues.[49,50]

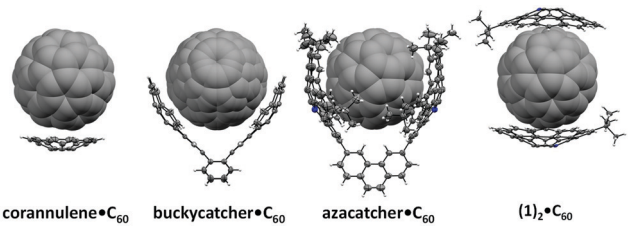

Fig. 1 Structures of selected buckybowl·C_{60} complexes.

[a] *Center for Multidimensional Carbon Materials (CMCM), Institute for Basic Science (IBS), Ulsan, 44919, Republic of Korea. E-mail: bielawski@unist.ac.kr*
[b] *Department of Chemistry, Ulsan National Institute of Science and Technology (UNIST), Ulsan, 44919, Republic of Korea*

† Electronic supplementary information (ESI) available: Synthetic procedures; additional titration data and binding isotherms; UV-vis and NMR spectra; cyclic voltammograms; X-ray crystallographic data for $(\mathbf{1})_2 \cdot C_{60}$; additional geometric measurements; DFT data. CCDC 2115565. For ESI and crystallographic data in CIF or other electronic format see DOI: https://doi.org/10.1039/d2cc01908f

An alternative approach to forming super-stoichiometric assemblies between buckybowls and fullerenes was envisioned. Although buckybowls generally feature smaller curvatures when compared to that of C_{60}, the binding affinity between two juxtaposed surfaces can be expected to increase as their curvatures become better matched. Moreover, complexation of an electron-rich buckybowl to C_{60} should result in charge transfer that effectively widens the curvature of the uncomplexed area of the fullerene. Such a process may increase the topological complementarity between the complexed C_{60} intermediate and a free buckybowl,[51] and thus may favor the formation of a super-stoichiometric complex. To test this hypothesis, an azacorannulene (**1**) which features a surface that is curved, electron-rich and mono-substituted to facilitate binding with C_{60} while maintaining a reasonably high degree of solubility was selected.[37] As will be described below, it was discovered that the azacorannulene not only forms a 2 : 1 complex with C_{60} in solution and in the solid-state but also binds to C_{60} with positive cooperativity as predicted by the hypothesis. Variable temperature titrations, calculations and structural models are also presented to gain a deeper understanding of the complex that formed and to clarify the unique binding phenomena. In a broader context, the discovery constitutes a new method for using allosteric changes to form super-stoichiometric complexes with fullerenes.

The intermolecular interactions formed between **1**, which was synthesized by modifying a literature[37] procedure (see ESI,† Scheme S1), and C_{60} were first probed through a series of titrations and monitored *via* ^{1}H NMR spectroscopy. Treating a solution of the buckybowl ($[\mathbf{1}]_0$ = 240 μM in toluene-d_8) with increasing quantities of C_{60} ($[C_{60}]_0$ = 2.5 mM) generally caused the ^{1}H NMR signals that were assigned to **1** to shift upfield although the signals assigned to the *tert*-butyl group and to the hydrogen atom located at the 2-position shifted downfield (Fig. 2a). The former chemical shifts can be attributed to shielding effects (*e.g.*, CH–π interactions), while the latter may be induced *via* interactions with the LUMO on C_{60} (*vide infra*). The systematic shift in signals indicated that a well-defined complex formed *in situ* as the two components were combined.[52]

A Job plot was constructed to determine the stoichiometry of the complex formed. A maximum was observed when the mole fraction of C_{60} was approximately one-third, consistent with the formation of a 2 : 1 complex (Fig. 2b).[53,54] To verify the stoichiometry and to measure the constituent association constants, binding isotherm data were plotted and analyzed with BindFit,[55] a non-linear regression analysis program. The binding isotherm featured an inflection point when the stoichiometry of the two components was 2 : 1 and then began to saturate (Fig. 2c). Likewise, good agreement between the binding isotherm data and a cubic fit that follows a 2 : 1 model (*i.e.*, $(\mathbf{1})_2{\cdot}C_{60}$) was obtained[56,57] and the association constants for the two binding events were determined to be K_1 = 2126 ± 87 M^{-1} and K_2 = 1359 ± 103 M^{-1}. The first binding event appeared to facilitate the second event as a cooperativity factor (α), defined as $4K_2/K_1$, of 2.56 was calculated for the system.[55]

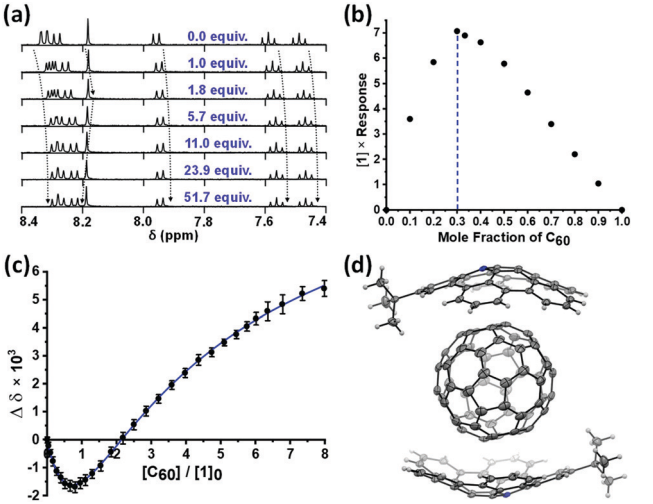

Fig. 2 (a) ^{1}H NMR spectra that were recorded as **1** (240 μM) was titrated with increasing quantities of C_{60} (2.5 mM) (indicated) in toluene-d_8 at 25 °C. (b) Job Plot used to determine the stoichiometry of the complex formed as obtained by measuring the response, defined as $|\Delta\delta| \times 10^6$, between **1** and C_{60} in toluene-d_8 at 25 °C. (c) Averaged binding isotherm data (black circles) with a 2 : 1 cubic fit (blue line) of the hydrogen assigned to the 2-position of **1**; conditions: $[\mathbf{1}]_0$ = 240 μM, $[C_{60}]_0$ = 2.5 mM, toluene-d_8, 25 °C. (d) ORTEP diagram of $(\mathbf{1})_2{\cdot}C_{60}$. Thermal displacement ellipsoids are drawn at the 50% probability level.

The overall affinity of **1** toward C_{60} can be calculated ($K_1 \times K_2$ = 2.8 × 10^6 M^{-2})[55,58,59] and compared to the values reported for the aforementioned molecular tweezers.[38] For reference, the self-association constants of **1** (2.4 ± 0.4 M^{-1})[37–60] and $(\mathbf{1})_2{\cdot}C_{60}$ (10.7 ± 2.9 M^{-1}) were measured in toluene-d_8 at 25 °C and determined to be relatively small. Collectively, the data indicated that a tight 2 : 1 complex formed between **1** and C_{60} and that the formation process occurred selectively and with positive cooperativity.

A van't Hoff analysis was performed to gain a deeper insight into the process that governs complex formation. The analysis indicated that the first binding event (*i.e.*, the formation of $\mathbf{1}{\cdot}C_{60}$) is enthalpy-driven and entropically disfavored (ΔH = −5.3 kcal mol^{-1}; ΔS = −3.0 cal mol^{-1} K^{-1}) which may be due in part to a loss in translational freedom. However, the intermediate complex (*i.e.*, $\mathbf{1}{\cdot}C_{60}$) appears to be preorganized toward binding additional **1** as the second binding event (*i.e.*, the formation of $(\mathbf{1})_2{\cdot}C_{60}$) was measured to be entropically favored (ΔS = +16.0 cal mol^{-1} K^{-1}) in accord with the hypothesis. The second step appears to incur an enthalpic penalty (ΔH = +0.65 kcal mol^{-1}) which may stem from a repulsive electrostatic interaction as the C_{60} component in the intermediate complex should be relatively electron-rich due to charge transfer. Support for this conclusion was obtained *via* cyclic voltammetry which revealed that $(\mathbf{1})_2{\cdot}C_{60}$ exhibited a lower reduction potential than the C_{60} host (E_{red} = −1.03 V *vs.* −1.00 V, respectively, in 5 : 1 v/v *o*-dichlorobenzene/acetonitrile) as well as a higher oxidation potential than its constituent guest (**1**) (E_{ox} = +0.37 V *vs.* +0.35 V, respectively). Additional support was obtained from the structural analyses and the calculations described below.

Further evidence that supported the formation of a 2:1 complex between **1** and C_{60} was obtained by a single-crystal X-ray diffraction analysis. The solid-state structure features a concave-convex relationship analogous to those observed in other types of buckybowl·fullerene complexes reported in the literature (Fig. 2d).[31,33,35] The bowl-to-ball (BtB) distance measured for $(\mathbf{1})_2{\cdot}C_{60}$ (6.88 Å) was intermediate of the values reported for the solid-state structures of (2,5,11,14-tetra-*tert*-butyl-6b^2-azapentabenzo[*bc*,*ef*,*hi*,*kl*,*no*]-corannulene)·C_{60} (6.82 Å)[35] and corannulene·C_{60} (6.94 Å).[31] The assembly angle (θ), which is defined as the angle between the center of C_{60} and the pyrrole centroids on **1**, was measured to be 180.0°, indicating that the two guests were antipodal. Inspection of the X-ray data revealed that every ring in **1** was within 4.0 Å of C_{60}, consistent with a π–π interaction,[61] and that the number of π–π contacts formed appeared to depend on the depth of the buckybowl. For example, while only one contact between the central ring of **1** and C_{60} was identified, an average of 1.6 and 1.4 contacts to C_{60} were measured for the inner and peripheral rings, respectively. A series of CH–π interactions in the crystal lattice were also identified and may serve to stabilize the crystal lattice or to guide packing (see ESI,† Fig. S50–S52).

A series of structural analyses were performed to assess shape complementarity and a summary is shown in Fig. 3.[62] Although a π-orbital axis vector[63,64] (POAV) angle of 8.28° has been reported for **1**,[37] the average POAV angle of the pyrrolyl carbons in $(\mathbf{1})_2{\cdot}C_{60}$ was wider (8.37°) and thus better matched with the angle reported for C_{60} (11.64°).[65] The remaining carbon atoms in the inner rings of the complex also displayed a larger average hybridization angle (3.02°) than that of virgin **1** (2.88°). The POAV differential resulted in a deeper bowl (c.f., the distance from the pyrrole centroid to the outermost carbon atoms in the buckybowl) of $(\mathbf{1})_2{\cdot}C_{60}$ (1.63 Å) when compared to that measured for **1** (1.58 Å).[37] Likewise, the eccentricity (e) of **1** was also measured to decrease upon complexation. In other words, the azacorannulene guests appeared to have flexed to better match the topology of the C_{60} host. The binding phenomena effectively compressed C_{60} into a prolate spheroid as the semi-minor (binding) axis (e = 0.000) of the host was shorter than its semi-major axis (e = 0.024). The average POAV angle calculated for the binding regions was also relatively acute (11.55°) when compared to that of uncomplexed C_{60}.[65]

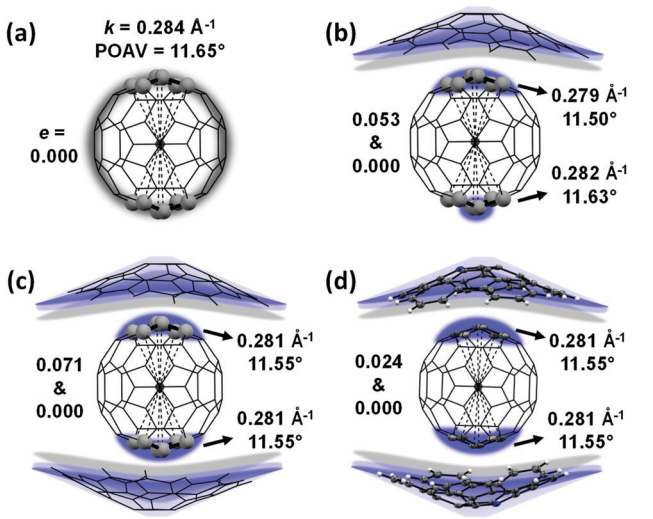

Fig. 3 Illustrations of the corresponding calculated changes in eccentricity $\left(e = \sqrt{1 - \frac{r^2_{\text{min or}}}{r^2_{major}}}\right)$, curvature $\left(k = \frac{2\sin(\theta_{\text{POAV}})}{\text{avg. bond length (Å)}}\right)$ and POAV values at different regions of C_{60} (shaded blue) as obtained from the (a–c) DFT or (d) X-ray crystal data. The eccentricity, curvature and POAV values for **1** are 0.948, 0.204 $Å^{-1}$ and 8.11°, respectively. The *tert*-butyl groups on **1** were omitted for clarity.

To obtain a deeper understanding of the supramolecular assembly process and the structures of the complexes that formed, a series of DFT calculations (M06-2X-D3/6-31G(d,p)) were conducted on C_{60}, **1**, **1**·C_{60} and $(\mathbf{1})_2{\cdot}C_{60}$. Good agreement between the X-ray data collected for $(\mathbf{1})_2{\cdot}C_{60}$ and the calculated data was realized. For example, the calculated assembly angle of the azacorannulene units (179.9°) and the BtB distance (6.73 Å) were consistent with the X-ray data. Key intermolecular charge-transfer interactions were also identified upon inspection of the structures calculated for $(\mathbf{1})_2{\cdot}C_{60}$ and **1**·C_{60}. The HOMO was found to reside on the azacorannulene units whereas the LUMO was located on C_{60}. The calculations showed that the first binding event effectively caused the opposite (open) region of the host to experience compression as the semi-minor axis of C_{60} in **1**·C_{60} (7.073 Å) was contracted when compared to that of virgin C_{60} (7.079 Å). A curvature value[65] (k) of 0.282 $Å^{-1}$ was calculated for the compressed region in **1**·C_{60}, which is more complementary to that measured for **1** (0.204 $Å^{-1}$). For reference, k values of 0.284 $Å^{-1}$ and 0.281 $Å^{-1}$ were calculated for uncomplexed C_{60} and the C_{60} contained in $(\mathbf{1})_2{\cdot}C_{60}$, respectively. Similarly, the POAV angle calculated for the open region in **1**·C_{60} was reduced and thus better matched the surface topology of **1**.

The subtleties of such stereoelectronically-induced, allosteric changes were borne out in the binding phenomena. As noted above, the K_1 value was measured to be larger than the K_2 value and the overall binding process was measured to proceed with positive cooperativity. Consistent with the experimental data, enthalpy of formation values of −31.8 and −30.8 kcal mol^{-1} were calculated for **1**·C_{60} and $(\mathbf{1})_2{\cdot}C_{60}$, respectively. The LUMO of **1**·C_{60} (−2.49 eV) was slightly higher in energy than that of C_{60} (−2.70 eV), which may explain why the second binding event is less favored than the first. The exposed surface of **1**·C_{60} is relatively electron-rich due to charge transfer and thus may disfavor binding to a second unit of (electron-rich) **1**. However, the electronic offset caused by the first binding event appears to be compensated by steric changes that effectively increase the topological complementarity between the binding partners.

In summary, it was demonstrated that two units of azacorannulene **1** bind to C_{60} in solution as well as in the solid-state. The binding phenomena proceed with high affinity and positive cooperativity as determined by titration experiments and DFT calculations. The binding of **1** to C_{60} results in charge-transfer and causes the fullerene to adopt a compressed

spheroid geometry. The stereoelectronic effect afforded an open site in the resulting $\mathbf{1}\cdot C_{60}$ intermediate that displayed increased shape complementarity to **1**, as indicated by a series of POAV and curvature analyses, and ultimately facilitated the second binding event. The allosteric changes were corroborated with an X-ray analysis as well as by a series of thermodynamic measurements and calculations. In a broader perspective, the design principles described should faciliate access to super-stoichiometric carbon assemblies with potential applications in carbon chemistry, materials science, and nanotechnology.

The IBS (R01-019-D1) is acknowledged for support.

Conflicts of interest

There are no conflicts to declare.

Notes and references

1 H. W. Kroto, J. R. Heath, S. C. O'Brien, R. F. Curl and R. E. Smalley, *Nature*, 1985, **318**, 162–163.
2 C. Z. Li, H. L. Yip and A. K.-Y. Jen, *J. Mater. Chem.*, 2012, **22**, 4161–4177.
3 G. Dennler, M. C. Scharber and C. J. Brabec, *Adv. Mater.*, 2009, **21**, 1323–1338.
4 D. M. Guldi, B. M. Illescas, C. M. Atienza, M. Wielopolskia and N. Martin, *Chem. Soc. Rev.*, 2009, **38**, 1587–1597.
5 E. Castro, A. H. Garcia, G. Zavala and L. Echegoyen, *J. Mater. Chem. B*, 2017, **5**, 6523–6535.
6 P. Anilkumar, F. Lu, L. Cao, P. G. Luo, J. H. Liu, S. Sahu, K. N. Tackett, Y. Wang and Y. P. Sun, *Curr. Med. Chem.*, 2011, **18**, 2045–2059.
7 F. Diederich and M. Gomez-Lopez, *Chem. Soc. Rev.*, 1999, **28**, 263–277.
8 T. Andersson, K. Nilsson, M. Sundahl, G. Westman and O. Wennerstrom, *J. Chem. Soc., Chem. Commun.*, 1992, 604–606.
9 N. Komatsu, *J. Inclusion Phenom. Macrocyclic Chem.*, 2008, **61**, 195–216.
10 S. S. Babu, H. Mohwald and T. Nakanishi, *Chem. Soc. Rev.*, 2010, **39**, 4021–4035.
11 T. Nakanishi, *Chem. Commun.*, 2010, **46**, 3425–3436.
12 Y. Shi, K. Cai, H. Xiao, Z. C. Liu, J. W. Zhou, D. K. Shen, Y. Y. Qiu, Q. H. Guo, C. Stern, M. R. Wasielewski, F. Diederich, W. A. Goddard and J. F. Stoddart, *J. Am. Chem. Soc.*, 2018, **140**, 13835–13842.
13 C. Garcia-Simon, M. Garcia-Borras, L. Gomez, T. Parella, S. Osuna, J. Juanhuix, I. Imaz, D. Maspoch, M. Costas and X. Ribas, *Nat. Commun.*, 2014, 5.
14 K. Nagata, E. Dejima, Y. Kikuchi and M. Hashiguchi, *Chem. Lett.*, 2005, **34**, 178–179.
15 Y. Shoji, K. Tashiro and T. Aida, *J. Am. Chem. Soc.*, 2010, **132**, 5928–5929.
16 T. Haino, E. Hirai, Y. Fujiwara and K. Kashihara, *Angew. Chem., Int. Ed.*, 2010, **49**, 7899–7903.
17 X. Zhang and M. Takeuchi, *Angew. Chem., Int. Ed.*, 2009, **48**, 9646–9651.
18 G. Fernandez, E. M. Perez, L. Sanchez and N. Martin, *J. Am. Chem. Soc.*, 2008, **130**, 2410–2411.
19 S. Barrau, T. Heiser, F. Richard, C. Brochon, C. Ngov, K. van de Wetering, G. Hadziioannou, D. V. Anokhin and D. A. Ivanov, *Macromolecules*, 2008, **41**, 2701–2710.
20 M. Schmittel, B. He and P. Mal, *Org. Lett.*, 2008, **10**, 2513–2516.
21 T. Haino, M. Yanase and Y. Fukazawa, *Angew. Chem., Int. Ed. Engl.*, 1997, **36**, 259–260.
22 S. Goeb and M. Salle, *Acc. Chem. Res.*, 2021, **54**, 1043–1055.
23 D. Canevet, M. Gallego, H. Isla, A. de Juan, E. M. Perez and N. Martin, *J. Am. Chem. Soc.*, 2011, **133**, 3184–3190.
24 R. Ziessel, G. Ulrich, K. J. Elliott and A. Harriman, *Chem. – Eur. J.*, 2009, **15**, 4980–4984.
25 Y. T. Wu and J. S. Siegel, *Top. Curr. Chem.*, 2014, **349**, 63–120.
26 J. Y. Zheng, K. Tashiro, Y. Hirabayashi, K. Kinbara, K. Saigo, T. Aida, S. Sakamoto and K. Yamaguchi, *Angew. Chem., Int. Ed.*, 2001, **40**, 1858–1861.
27 T. Kawase and H. Kurata, *Chem. Rev.*, 2006, **106**, 5250–5273.
28 M. Yanney, F. R. Fronczek and A. Sygula, *Angew. Chem., Int. Ed.*, 2015, **54**, 11153–11156.
29 J. W. Steed, P. C. Junk, J. L. Atwood, M. J. Barnes, C. L. Raston and R. S. Burkhalter, *J. Am. Chem. Soc.*, 1994, **116**, 10346–10347.
30 W. E. Barth and R. G. Lawton, *J. Am. Chem. Soc.*, 1971, **93**, 1730–1745.
31 L. N. Dawe, T. A. AlHujran, H. A. Tran, J. I. Mercer, E. A. Jackson, L. T. Scotc and P. E. Georghiou, *Chem. Commun.*, 2012, **48**, 5563–5565.
32 W. Xiao, D. Passerone, P. Ruffieux, K. Ait-Mansour, O. Groning, E. Tosatti, J. S. Siegel and R. Fasel, *J. Am. Chem. Soc.*, 2008, **130**, 4767–4771.
33 P. E. Georghiou, A. H. Tran, S. Mizyed, M. Bancu and L. T. Scott, *J. Org. Chem.*, 2005, **70**, 6158–6163.
34 S. Mizyed, P. E. Georghiou, M. Bancu, B. Cuadra, A. K. Rai, P. C. Cheng and L. T. Scott, *J. Am. Chem. Soc.*, 2001, **123**, 12770–12774.
35 H. Yokoi, Y. Hiraoka, S. Hiroto, D. Sakamaki, S. Seki and H. Shinokubo, *Nat. Commun.*, 2015, **6**, 1–9.
36 M. Saito, H. Shinokubo and H. Sakurai, *Mater. Chem. Front.*, 2018, **2**, 635–661.
37 S. Ito, Y. Tokimaru and K. Nozaki, *Angew. Chem., Int. Ed.*, 2015, **54**, 7256–7260.
38 M. Takeda, S. Hiroto, H. Yokoi, S. Lee, D. Kim and H. Shinokubo, *J. Am. Chem. Soc.*, 2018, **140**, 6336–6342.
39 A. Sygula, F. R. Fronczek, R. Sygula, P. W. Rabideau and M. M. Olmstead, *J. Am. Chem. Soc.*, 2007, **129**, 3842–3843.
40 V. H. Le, M. Yanney, M. McGuire, A. Sygula and E. A. Lewis, *J. Phys. Chem. B*, 2014, **118**, 11956–11964.
41 M. M. Olmstead, D. A. Costa, K. Maitra, B. C. Noll, S. L. Phillips, P. M. Van Calcar and A. L. Balch, *J. Am. Chem. Soc.*, 1999, **121**, 7090–7097.
42 X. S. Ke, T. Kim, J. T. Brewster, V. M. Lynch, D. Kim and J. L. Sessler, *J. Am. Chem. Soc.*, 2017, **139**, 4627–4630.
43 Y. H. Yang, K. M. Cheng, Y. Lu, D. D. Ma, D. H. Shi, Y. X. Sun, M. Y. Yang, J. Li and J. F. Wei, *Org. Lett.*, 2018, **20**, 2138–2142.
44 Y. Y. Xu, H. R. Tian, S. H. Li, Z. C. Chen, Y. R. Yao, S. S. Wang, X. Zhang, Z. Z. Zhu, S. L. Deng, Q. Y. Zhang, S. F. Yang, S. Y. Xie, R. B. Huang and L. S. Zheng, *Nat. Commun.*, 2019, **10**, 1–9.
45 A. S. Filatov, M. V. Ferguson, S. N. Spisak, B. Li, C. F. Campana and M. A. Petrukhina, *Cryst. Growth Des.*, 2014, **14**, 756–762.
46 H. Yokoi, S. Hiroto, D. Sakamaki, S. Seki and H. Shinokubo, *Chem. Sci.*, 2018, **9**, 819–824.
47 Y. Saegusa, T. Ishizuka, T. Kojima, S. Mori, M. Kawano and T. Kojima, *Chem. – Eur. J.*, 2015, **21**, 5302–5306.
48 P. L.-A. Kuragama, F. R. Fronczek and A. Sygula, *Org. Lett.*, 2015, **17**, 5292–5295.
49 F. Hof, S. L. Craig, C. Nuckolls and J. Rebek, *Angew. Chem., Int. Ed.*, 2002, **41**, 1488–1508.
50 J. Rebek, *Acc. Chem. Res.*, 1984, **17**, 258–264.
51 A. S. Filatov, E. A. Jackson, L. T. Scott and M. A. Petrukhina, *Angew. Chem., Int. Ed.*, 2009, **48**, 8473–8476.
52 Isosbestic points were observed at 425 and 625 nm upon titrating C_{60} with **1** and provided further support that a well-defined complex was formed (see ESI,† Fig. S35).
53 D. B. Hibbert and P. Thordarson, *Chem. Commun.*, 2016, **52**, 12792–12805.
54 F. Ulatowski, K. Dabrowa, T. Balakier and J. Jurczak, *J. Org. Chem.*, 2016, **81**, 1746–1756.
55 P. Thordarson, *Chem. Soc. Rev.*, 2011, **40**, 5922–5923.
56 The differences between the model and the recorded data were plotted and found to be small (see ESI,† Fig. S31).
57 Consistent with complexation, the diffusion coefficient of $(\mathbf{1})_2\cdot C_{60}$ (6.54×10^{-10} m^2 s^{-1}) was smaller than that of **1** (7.43×10^{-10} m^2 s^{-1}) (see ESI,† Fig. S36, S37 and Table S9).
58 K. A. Connors, *Binding constants: the measurement of molecular complex stability*, Wiley, New York, 1987.
59 L. K.-S. von Krbek, C. A. Schalley and P. Thordarson, *Chem. Soc. Rev.*, 2017, **46**, 2622–2637.
60 A similar self-association constant (5.0 ± 0.4 M^{-1}) was reported[37] for **1** in deuterated benzene at 25 °C.
61 C. A. Hunter and J. K.-M. Sanders, *J. Am. Chem. Soc.*, 1990, **112**, 5525–5534.
62 More details are in the ESI;† see Fig. S53–S58 and Tables S17–S23.
63 R. C. Haddon, *J. Phys. Chem. A*, 2001, **105**, 4164–4165.
64 R. C. Haddon, *J. Am. Chem. Soc.*, 1986, **108**, 2837–2842.
65 R. C. Haddon, *J. Am. Chem. Soc.*, 1997, **119**, 1797–1798.